Benchtop quantification of gutter formation and compression of chimney stent grafts in relation to renal flow in chimney endovascular aneurysm repair and endovascular aneurysm sealing configurations

Johannes T. Boersen, MSc,[a,b,c] Esme J. Donselaar, MD,[a] Erik Groot Jebbink, MSc,[a,c] Roeliene Starreveld, MSc,[a,c] Simon P. Overeem, MSc,[b,c] Cornelis H. Slump, PhD,[c] Jean-Paul P. M. de Vries, MD, PhD,[b] *and* Michel M. P. J. Reijnen, MD, PhD,[a] *Arnhem, Nieuwegein, and Enschede, The Netherlands*

ABSTRACT

Background: The chimney technique has been successfully used to treat juxtarenal aortic aneurysms. The two main issues with this technique are gutter formation and chimney graft (CG) compression, which induce a risk for type Ia endoleaks and stent thrombosis, respectively. In this benchtop study, the geometry and renal artery flow of chimney endovascular aneurysm repair configurations were compared with chimney configurations with endovascular aneurysm sealing (ch-EVAS).

Methods: Seven flow phantoms were constructed, including one control and six chimney endovascular aneurysm repairs (Endurant [Medtronic Inc, Minneapolis, Minn] and AFX [Endologix Inc, Irvine, Calif]) or ch-EVAS (Nellix, Endologix) configurations, combined with either balloon-expandable or self-expanding CGs with an intended higher positioning of the right CG in comparison to the left CG. Geometric analysis was based on measurements at three-dimensional computed tomography angiography and included gutter volume and CG compression, quantified by the ratio between maximal and minimal diameter (D-ratio). In addition, renal artery flow was studied in a physiologic flow model and compared with the control.

Results: The average gutter volume was 343.5 ± 142.0 mm^3, with the lowest gutter volume in the EVAS-Viabahn (W. L. Gore & Associates, Flagstaff, Ariz) combination (102.6 mm^3) and the largest in the AFX-Advanta V12 (Atrium Medical Corporation, Hudson, NH) configuration (559.6 mm^3). The maximum D-ratio was larger in self-expanding CGs than in balloon-expandable CGs in all configurations (2.02 ± 0.34 vs 1.39 ± 0.13). The CG compression had minimal influence on renal volumetric flow (right, 390.7 ± 29.4 mL/min vs 455.1 mL/min; left, 423.9 ± 28.3 mL/min vs 410.0 mL/min in the control).

Conclusions: This study showed that gutter volume was lowest in ch-EVAS in combination with a Viabahn CG. CG compression was lower in configurations with the Advanta V12 than with Viabahn. Renal flow is unrestricted by CG compression. (J Vasc Surg 2017;66:1565-73.)

Clinical Relevance: Chimney endovascular aneurysm repair and chimney endovascular aneurysm sealing are used more commonly for elective repair of juxtarenal abdominal aortic aneurysms. Gutter formation and chimney graft compression may occur because of a mismatch in architecture between the chimney stent grafts and the endograft or endosystem, and this may induce a risk for complications such as type Ia endoleaks and stent thrombosis. This benchtop study evaluated gutter formation and chimney stent graft compression for various chimney endovascular aneurysm repair and chimney endovascular aneurysm sealing configurations in relation to renal flow.

Endovascular aneurysm repair (EVAR) has become the standard treatment for abdominal aortic aneurysm (AAA) because of an improved 30-day outcome and a shorter rehabilitation period compared with open repair.[1] EVAR has proven long-term durability when it is used on label.[2] Applicability of EVAR is mostly limited by unfavorable proximal neck characteristics, including short (<15 mm) or severely angulated (>60 degrees) infrarenal necks, and dilations that involve the juxtarenal aorta, present in around 20% of patients.[3] These characteristics are associated with a substantial risk for adverse events after EVAR, including migration and type Ia

From the Department of Surgery, Rijnstate Hospital, Arnhem[a]; the Department of Vascular Surgery, St. Antonius Hospital, Nieuwegein[b]; and the MIRA Research Institute for Biomedical Technology and Technical Medicine, University of Twente, Enschede.[c]

Funding for this study was obtained from Medtronic Inc (Minneapolis, Minn), Endologix Inc (Irvine, Calif), and Atrium Maquet (Atrium Medical Corporation, Hudson, NH).

Author conflict of interest: M.M.R. is a consultant for Endologix. J.-P.V. is a consultant for Endologix and Medtronic.

Additional material for this article may be found online at www.jvascsurg.org.

Correspondence: Johannes T. Boersen, MSc, Department of Vascular Surgery, St. Antonius Hospital, Koekoekslaan 1, 3430 EM Nieuwegein, The Netherlands (e-mail: j.boersen@antoniusziekenhuis.nl).

The editors and reviewers of this article have no relevant financial relationships to disclose per the JVS policy that requires reviewers to decline review of any manuscript for which they may have a conflict of interest.

0741-5214

http://dx.doi.org/10.1016/j.jvs.2016.10.058

endoleaks.[4,5] Fenestrated EVAR (FEVAR) has been demonstrated to be an alternative treatment option for this group of patients, with good short- and intermediate-term outcomes.[3,6] However, anatomic characteristics may preclude the use of custom-made devices, the construction is expensive, and the technique is unsuitable for ruptured AAA repair because of 4 to 6 weeks of manufacturing.[7,8] Moreover, these devices are not globally available.

Chimney EVAR (ch-EVAR), in which a standard modular graft is combined with chimney, or parallel, stent grafts (CGs) to maintain flow in side branches (ie, renal arteries, superior mesenteric artery [SMA], and celiac trunk), provides an off-the-shelf solution in patients with a juxtarenal AAA[9] with a 30-day mortality rate comparable to that of FEVAR.[7,10] However, ch-EVAR has been associated with a higher incidence of stroke and early type Ia endoleaks in comparison to FEVAR.[7] Moreover, a difference in stent geometry and architecture (ie, material stiffness) of standard modular grafts and CGs may result in gutter formation (GF) and induce a risk for early type Ia endoleaks. In addition, compression or kinking of the CG may be caused by the radial force of the endograft that occurs from oversizing of the endograft in the aortic neck. CG compression is supposed to influence renal flow (ie, volumetric flow rate, flow profile), and changes in flow profile may induce a risk for thrombosis.

Endovascular aneurysm sealing (EVAS) is an alternative technique for AAA repair, obliterating the aneurysm sac by polymer filling of endobags that surround dual cobalt-chromium endoframes.[11] EVAS was designed to reduce the incidence of migration and endoleaks, and according to the instructions for use, AAAs with an infrarenal neck length of >10 mm can be treated with EVAS.[12] Its potential has also been demonstrated in combination with chimneys (ch-EVAS) in several case reports in both an elective and an acute setting.[13-15] The endobags potentially allow a better conformation to the CG geometry after ch-EVAS, which could reduce the incidence of gutters and subsequent type Ia endoleaks in comparison to ch-EVAR. In addition, after curing of the polymer, the filled endobags will no longer compete with the radial strength of the CG, in contrast to the situation after ch-EVAR.

In this benchtop research, the geometry of several ch-EVAR and ch-EVAS configurations was studied, including CG compression and GF. In addition, volumetric flow for each CG was measured.

METHODS

Flow phantoms and stents. Flow phantom geometry was based on an average aortoiliac anatomy of 25 elective juxtarenal AAA patients, performed at preoperative computed tomography (CT) scans, including a short proximal neck (aneurysm starting at a distance of 10 mm) and branches of the SMA, renal arteries, and common iliac arteries (Table I). The infrarenal neck morphology was reverse tapered with an infrarenal neck diameter of 26 mm and a linear increase to 38 mm over a distance of 15 mm. The manufacturing of seven juxtarenal AAA flow phantoms was conducted by Elastrat (Geneva, Switzerland). One model was used as a reference without stents, and the others were used to implant six different CG configurations, including EVAR with Endurant II (ETBF 32 16 C 166 EE; ETLW 16 16 C 124 EE; Medtronic Inc, Minneapolis, Minn) and AFX (BA28-70/116-30; A34-34/C100-020V; Endologix Inc, Irvine, Calif) and EVAS with Nellix (Nx-10-150, Endologix) combined with either balloon-expandable Atrium Advanta V12 (known as iCast in the United States; 6 × 58 mm; Atrium Medical Corporation, Hudson, NH) or self-expanding Gore Viabahn (6 × 38 mm; W. L. Gore & Associates, Flagstaff, Ariz) CGs. The proximal graft diameter of the EVAR devices was 32 mm and 34 mm for the Endurant and AFX, respectively. This size resulted in 23.7% and 30.7% oversizing for the Endurant and AFX endografts, respectively.

Implantation in the models was performed by two experienced vascular surgeons (J.-P.V., M.M.R.). The intended position of the endograft was at the distal

Table I. Model geometries

Suprarenal aorta		
Diameter, mm		26
Length, mm		65
Angulation, degrees		0
SMA		
Diameter, mm		8
Length, mm		120
Takeoff angle, degrees		60
Renal arteries	Right	Left
Diameter, mm	5	5
Length, mm	120	120
Takeoff angle, degrees	111	115
Infrarenal aorta		
Diameter, mm		
Infrarenal neck, mm		26
Baseline, mm		26
Baseline + 15 mm, mm		38
Maximum AAA, mm		50
Aortic bifurcation, mm		26
Length, mm		105
Angulation, degrees		0
Common iliac arteries	Right	Left
Diameter, mm	12	12
Length, mm	130	130
Takeoff angle, degrees	27	23

AAA, Abdominal aortic aneurysm; *SMA*, superior mesenteric artery.
The model geometry was based on an average AAA anatomy of 25 elective patients with a juxtarenal aortic aneurysm.

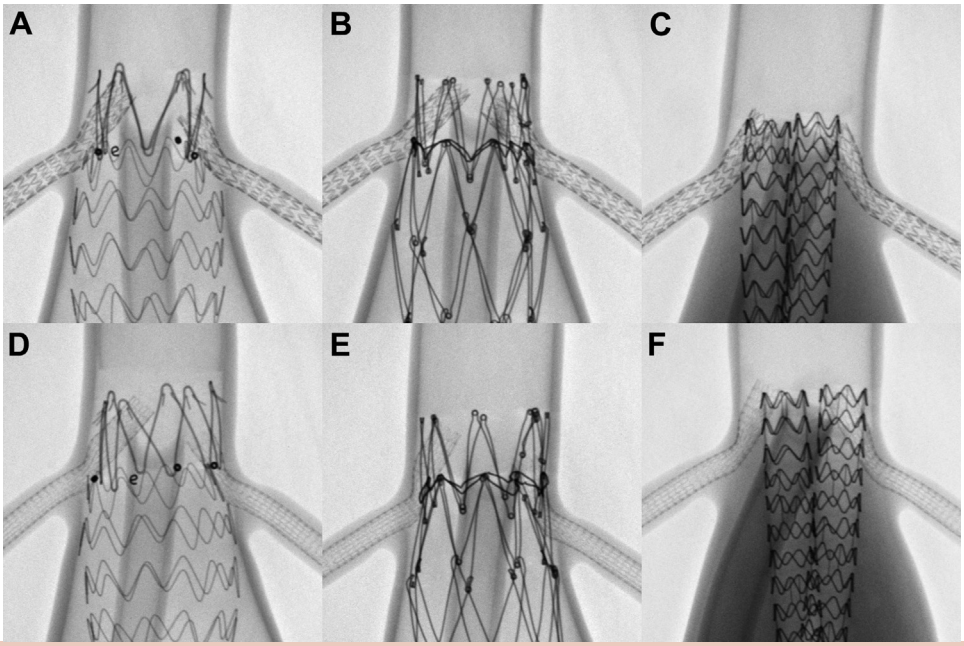

Fig 1. Anteroposterior view of the benchtop chimney stent graft (CG) configurations. **A,** Endovascular aneurysm repair (EVAR), Endurant with Advanta V12. **B,** EVAR, Endurant with AFX with Advanta V12. **C,** Nellix endovascular aneurysm sealing (EVAS) with Advanta V12. **D,** EVAR, Endurant with Gore Viabahn. **E,** EVAR, AFX with Gore Viabahn. **F,** Nellix EVAS with Gore Viabahn.

edge of the SMA (proximal end of the bare stent at the proximal edge of the SMA in the EVAS configurations). The intended positions of the proximal end of the right and left chimney were at the top and mid SMA, respectively, to study the influence of positioning on CG compression and GF (Figs 1 and 2). CGs were deployed in advance of the endograft main body or EVAS endobags to allow maximal expansion before eventual compression by the endograft. The proximal fixation zone of the EVAR devices was postdilated with a compliant balloon (Reliant, Medtronic) to minimize GF in these configurations, with 6-mm balloons in the CGs inflated. Similarly, polymer filling of the endobags was performed with balloons inflated in the CGs. Polymer fill volume of the EVAS endobags was 150 mL and 145 mL, respectively, for the Advanta V12 and Viabahn configurations, with an intended fill pressure of 180 mm Hg (186 mm Hg and 190 mm Hg). After stent deployment, the models were flushed with water with a temperature of ±37°C to allow maximal expansion of the nitinol stents. In addition, the EVAS configurations were stored in a 5% sodium solution to prevent degradation of the polymer.

Geometry analysis. Measurements of the stent configurations were performed with 3mensio Vascular (Pie Medical, Bilthoven, The Netherlands) in three dimensions at CT angiography. High-resolution CT scans were acquired with a 256-slice CT scanner (Brilliance iCT; Philips Healthcare, Eindhoven, The Netherlands). Scan parameters included a tube voltage of 120 kV, tube current time product of 250 mAs, increment of 0.75 mm, pitch of 0.25, and collimation of 12.5 mm × 0.625 mm. CT scans were reconstructed with a slice thickness of 0.67 mm. The models were scanned without filling with contrast material to enhance the contrast between the endobags and flow lumen in the EVAS models.

Gutter was defined as the volume between graft fabric and aortic wall in the aortic neck (15-mm distance between the distal-edge SMA to 10 mm from the lowermost renal artery). Gutter volume was calculated by the sum (ie, integral) of gutter area determined at subsequent CT slices at 2-mm distances. The start of the sealing zone was determined by the proximal stent markers for the EVAR configurations and 1 cm from the proximal stent strut for the EVAS configurations where the endobags actually fill with polymer. Measurements of gutter area were conducted using the functionality *polygon region of interest* in the software, including a surface calculation based on an interpolation algorithm between user-defined spline points to mark the boundaries of a gutter. Measurements were conducted in the plane perpendicular to the flow lumen, established by a center luminal line through the endograft flow lumen or the center of the endobags in the EVAS configurations (Fig 3, *A*).

CG compression was determined by the maximal deformation of the graft lumen calculated by the ratio between major axis and minor axis of the graft luminal area (D-ratio). The D-ratio is equal to 1 in case of a circular

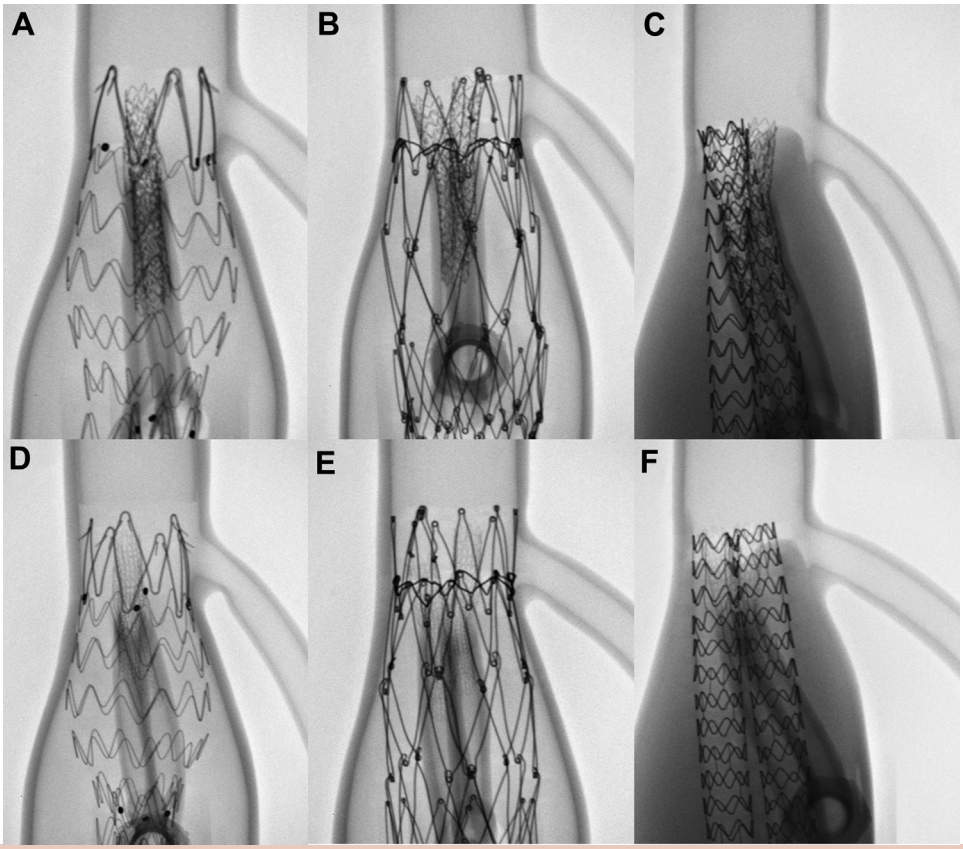

Fig 2. Lateral view of the benchtop chimney stent graft (CG) configurations. **A,** Endovascular aneurysm repair (EVAR), Endurant with Advanta V12. **B,** EVAR, AFX with Advanta V12. **C,** Nellix endovascular aneurysm sealing (EVAS) with Advanta V12. **D,** EVAR, Endurant with Gore Viabahn. **E,** EVAR, AFX with Gore Viabahn. **F,** Nellix EVAS with Gore Viabahn.

lumen area and becomes larger when eccentricity of the stent luminal area increases (ie, describes an ellipse). Major and minor axes of the graft luminal area were determined from the CG luminal area perpendicular to the flow lumen of the CG (Fig 3, *B*). Measurements were taken at subsequent CT slices at 2-mm distance. In addition, maximum CG angulation was determined with use of digital calipers over the central luminal line (*tortuosity* in 3mensio) of the CG (Fig 3, *C*). The measurements were performed two times by two experienced users to determine repeatability of measurements (J.T.B., R.S.). The outcomes were displayed by mean and standard deviation.

Flow measurements. The flow setup reported by Groot Jebbink et al was used to perform the flow experiments, including an additional connector for the SMA.[16] The model was based on a second-order Windkessel, including a compliance chamber to include peripheral artery impedance. Flow tests were conducted at physiologic rest conditions, including a volumetric flow rate of 2 L/min at 60 beats/min (peak flow 3.9 L/min) and an intended systemic pressure in a range of 120/80 mm Hg.[17] The outflow of each branch was controlled by needle valves with an equal outflow of 400 mL/min to each branch, including connections for the SMA and right and left renal artery and one connection for the common iliac arteries. A baseline resistance for each branch was determined by an equal branch flow for the aneurysm model, and this resistance was sustained throughout flow tests with the stented models. The volumetric flow rate was recorded with ultrasonic flow sensors (Cynergy3, type UF8B; Cynergy3 Components Ltd, Dorset, UK) two times for a duration of 30 seconds. The average flow, based on two recordings, was calculated for each branch and compared with the baseline. A blood-mimicking fluid, based on a ratio of 56% and 44% of glycerol and water contents, was used to obtain a fluid viscosity comparable to blood.[18]

Statistical analysis. The statistical analysis was performed with IBM SPSS Statistics (SPSS version 21; IBM Corp, Armonk, NY). Interobserver agreement of CT measurements was assessed with an interobserver reliability test, based on a two-way mixed model and absolute agreement between single measurements. The intraclass correlation coefficient (ICC) and 95% confidence interval were displayed for all measurements, and an

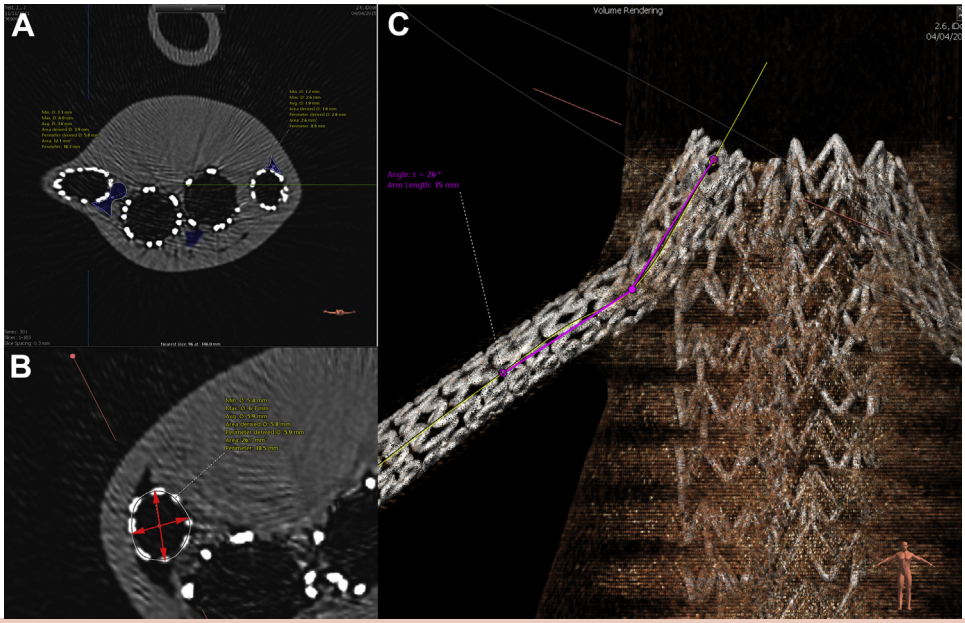

Fig 3. Measurements in 3mensio. **A,** Gutter area measurement in plane perpendicular to the endograft flow lumen. The gutter areas are displayed in *blue*. **B,** Chimney graft (CG) luminal area measurements in plane perpendicular to CG flow lumen. The *arrows* indicate the major and minor axes of the luminal area. **C,** Maximum angulation of CG measured with use of digital calipers over the central luminal line with the tortuosity tool.

Table II. Geometry analysis

	Endurant-Advanta V12	Endurant-Viabahn	AFX-Advanta V12	AFX-Viabahn	Nellix-Advanta V12	Nellix-Viabahn
Gutter volume, mm^3	367.6	220.0	559.6	319.4	382.2	102.6
Right CG geometry						
Maximum D-ratio	1.55	1.83	1.16	2.48	1.45	1.63
Maximum angulation, degrees	21.0	15.0	20.0	37.0	29.0	32.0
Left CG geometry						
Maximum D-ratio	1.37	2.03	1.35	2.36	1.43	1.76
Maximum angulation, degrees	30.0	29.0	15.0	36.0	24.0	32.0

CG, Chimney graft.
The maximum compression ratio (D-ratio) and angulation (degrees) are shown for right and left CG. In addition, gutter volume (mm^3) is displayed for each chimney stent graft configuration.

ICC > 0.7 was considered good agreement between the observers.

RESULTS

Geometry analysis. Measurement outcomes for each CG configuration are displayed in Table II. The average gutter volume was 343.5 ± 142.0 mm^3, and gutter volume appeared larger in the configurations with the Advanta V12 (367.6-559.6 mm^3) than in the configurations with the Viabahn (102.6-319.4 mm^3). The lowest gutter volume was found in the EVAS configurations with Viabahn stents (102.6 mm^3) and the largest in the AFX configurations with Advanta V12 stents (559.6 mm^3). In both EVAR and EVAS configurations, the CG compression was larger for Viabahn stents in comparison to Advanta V12 CGs (average D-ratio of 2.02 ± 0.34 vs 1.39 ± 0.13). CG compression of the Advanta V12 stents was similar between EVAR and EVAS configurations, whereas the compression of the Viabahn was less in the EVAS configuration in comparison to the EVAR configurations (Fig 4). The largest D-ratio over the entire stent length was found in the right chimney of the AFX model with Viabahn stent grafts (maximum D-ratio of 2.48), and the lowest D-ratio was found for the right CG in the AFX

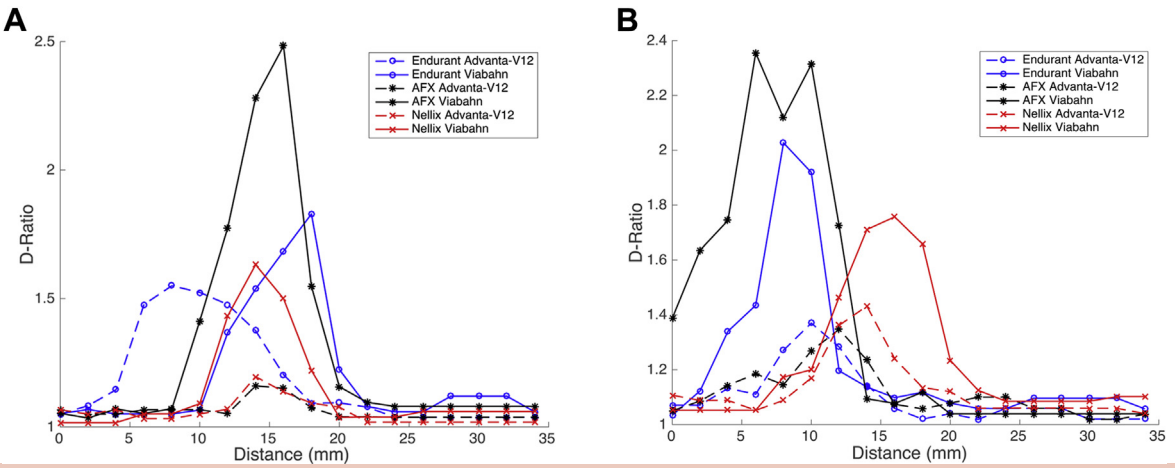

Fig 4. D-ratio of chimney grafts (CGs) for the different configurations. **A,** Right chimney. **B,** Left chimney. The start of each curve refers to the proximal graft end in the suprarenal aorta.

configuration with Advanta V12 stents (maximum D-ratio of 1.16). Maximum angulation of the CG appeared comparable between the different configurations (right, 25.7 ± 8.3 degrees; left, 27.7 ± 7.3 degrees), with a lower maximum angulation of balloon-expandable CGs in comparison to self-expanding CGs (balloon-expandable, 23.2 ± 5.7 degrees; self-expanding, 30.2 ± 8.0 degrees).

All measurements showed good interobserver agreement (Table III), all presenting an ICC > 0.7.

Flow. The average volumetric flow at the model inlet was in a physiologic range around 1.92 ± 0.05 L/min, as was the system pressure for all flow tests with a system pressure in a range of 115 to 135 mm Hg. The baseline flow through the SMA was lower than intended in the aneurysm model (292.4 mL/min on average vs intended branch flow of 400 mL/min), whereas the flow of the other branches was higher (right renal artery, 455.1 mL/min; left renal artery, 410.0 mL/min; common iliac artery, 949.2 mL/min). Right renal flow decreased on average in the chimney configurations (390.7 ± 29.4 mL/min vs 455.1 mL/min in the control), whereas left renal flow showed an increase (423.9 ± 28.3 mL/min vs 410.0 mL/min in the control). The average branch flow (SMA, renal and common iliac arteries) for each configuration is provided in the Supplementary Fig (online only). In addition, the SMA and common iliac artery flow appeared comparable between the unstented and stented configurations (on average 335.3 ± 36.4 mL/min vs 292.4 mL/min and 900.3 ± 44.8 mL/min vs 949.2 mL/min of flow through the SMA and common iliac artery in comparison to the control).

Table III. Interobserver variability of the computed tomography (CT) measurements

	ICC	95% Confidence interval	
		Lower	Upper
Diameter (n = 312)	0.937	0.845	0.967
Area (n = 312)	0.915	0.492	0.970
Angulation (n = 12)	0.953	0.848	0.986
Gutter volume (n = 6)	0.930	0.804	0.977

ICC, Intraclass correlation coefficient.

DISCUSSION

In this study, we have shown that gutter volume is lowest in ch-EVAS in combination with Viabahn as CG, probably because of good conformability of the endobags to the CG and vice versa. The maximum D-ratio was larger for self-expanding than for balloon-expandable CGs, indicating a higher compression rate. This difference is most likely caused by a difference in stent architecture between the Viabahn and Advanta V12 stents (nitinol vs stainless steel stents). Self-expanding stents usually have more resistance to radial compression than balloon-expandable stents and could therefore be more prone to stent deformation between the endograft and the aortic wall; however, they might conform better to the anatomy. A lower deformation of the Viabahn in the ch-EVAS configuration in comparison to the Viabahn ch-EVAR configurations may be due to an ongoing outward force of the EVAR device, which is not present in EVAS, after curing of the polymer. In addition, the angulation of the CG could cause stent deformation and a diameter reduction, as may squeezing of the stent between the proximal bare-metal struts in the EVAR configurations. Flow to visceral branches (SMA, renal arteries, and common iliac arteries) remained nearly unchanged. Slight changes in flow between right and left chimney may be due to a slightly larger maximal luminal area reduction of the right chimney in comparison to the left chimney in all configurations.

To date, limited evidence is available concerning the outcome of various combinations of EVAR devices and CGs for treatment of juxtarenal AAA, and the ideal combination is yet unknown. Decision-making is mostly

based on local experience with the various devices and preference of the surgeon. Benchtop research of CG configurations may help to differentiate between favorable and less favorable combinations of stents and to assess which combinations lead to potentially unfavorable geometries, such as CG compression and GF, which could lead to complications and subsequent reinterventions.

GF was larger in configurations with balloon-expandable stents than in the configurations with self-expanding stents, which confirms results of previous benchtop studies.[19-21] Absolute values for GF unfortunately are incomparable between studies because different methods were used to measure the gutter, including two-dimensional measurements of gutter area at multiple levels and three-dimensional measurements of gutter volume, including the entire volume of the gutters. The method that was used in the current study demonstrated good interobserver agreement and was comparable to the method that was used by Niepoth et al.[17] The results of the current study showed lower gutter volumes in the ch-EVAS configurations in comparison to the results from Niepoth et al (440-530 mm^3 vs 102.6-382.2 mm^3). This difference is most likely to the proximal sealing zone of the endobags, defined at 10 mm from proximal stent strut in the present study vs 5 mm by Niepoth at al. The present study demonstrated larger compression of Viabahn compared with the Advanta V12 stents in both ch-EVAR and ch-EVAS configurations. This has also been shown by others, examining geometry of CGs in ch-EVAR with the Endurant and Gore Excluder (W. L. Gore & Associates) endografts.[19,20] In contrast, Niepoth et al[21] demonstrated less compression of the Viabahn in comparison to the Advanta V12 in ch-EVAS configurations (42% vs 22%). Tran et al[22] showed that the diameter reduction in CG is consistently 10% to 15% larger at the junctional area than in other regions of the CG (proximal and distal). In the present study, the maximum angulation of the CGs was fairly low for Advanta V12 and Viabahn EVAS configurations, and a more parallel configuration with a sharper curve of the CG as presented by Niepoth et al may have resulted in larger deformation in the Advanta V12 in comparison to the Viabahn. The Viabahn may allow better conformation and may be more flexible to conform to more complex trajectories, including severe angulations.

The largest gutters were observed in the AFX configurations. In EVAR, sealing is obtained by oversizing of the graft with reference to the aortic wall. Mestres et al highlighted the importance of proper sizing of the endograft to minimize GF and to obtain the best possible sealing in ch-EVAR.[19] The best outcomes in terms of GF and CG compression were obtained by oversizing the endograft by 30%, although this is influenced by the number of required CGs. The oversizing of the main body was in a range of 20% to 30% for the ch-EVAR configurations. In addition, wall apposition and GF in ch-EVAR may be influenced by unpredictable deployment of the CGs because of interaction with the proximal bare-metal stent extension. The AFX has a greater number of proximal bare-metal stent struts, and this may provide less space to accommodate the CGs in comparison to the Endurant, in particular in combination with balloon-expandable CGs (Fig 1). However, the configurations were studied at static CT acquisitions, excluding the AFX active seal design feature with the graft material on the outside, which potentially may reduce the risk of type Ia endoleak in case of GF. This phenomenon could not be evaluated in the current study design. Gutter volume was the lowest in the Viabahn ch-EVAS configuration, with probably good conformability of both endosystem and CG. In ch-EVAS, sealing and potential GF depend on proper filling of the endobags in the proximal neck and conformation to the CGs. Moreover, additional balloons are required for balloon inflation of the CG during curing of the polymer, and CG compression was higher with Viabahn. Accordingly, the configurations with Endurant-Advanta V12 and EVAS-Advanta V12 may have acceptable GF.

This study showed GF in all configurations, and this may be inherent to the chimney technique. However, it is supposed that not all gutters will lead to type Ia endoleaks in vivo. In clinical practice, most gutters may be missed because of poor scan quality and poor filling of the gutter with contrast material. A small gutter with adequate sealing below the CG may exhibit a low risk for type Ia endoleaks after both ch-EVAR and ch-EVAS and may resolve over time by filling with thrombus. A longer gutter, originating at the proximal sealing zone and continuing until the aneurysm sac, may have a higher risk to cause a type Ia endoleak.[23]

The observed CG compression ratios for self-expanding and balloon-expandable stents had only a minimal influence on the measured renal artery volumetric flow. However, it is assumed that CG compression should be intended as low as possible because a complex shape (ie, asymmetric) of the CG luminal area may lead to unfavorable flow profiles and may induce a risk for stent thrombosis. The diameter of the renal artery branch was 5 mm, and therefore a CG with a diameter of 6 mm was used. A larger CG diameter may result in more CG compression.[20]

Another serious limitation of the chimney technique is a significantly higher incidence of stroke compared with standard EVAR and FEVAR procedures, in which fenestrations can be managed through femoral access. The reported incidence for stroke has been 3.2% for ch-EVAR vs 0.3% for FEVAR.[7] Also, the incidence of early type Ia endoleaks is higher with the ch-EVAR technique in comparison to FEVAR (10% vs 4.3%).[7]

Limitations. The used phantom had a relatively short proximal sealing zone as the distance between the distal edge of the SMA and the lowest renal artery was only 12 mm. This length was considered healthy aortic neck, and the stent sizing was based on the aortic diameter in this part. Accordingly, based on a minimum oversizing of 20% for proper endograft fixation in the aortic neck, the total length of sealing zone was at maximum 15 mm as the aortic diameter starts to increase below the renal arteries. The positioning accuracy of the stent grafts was not assessed in this study, and a lower positioning may cause differences in GF and CG compression, in particular in a short neck anatomy. Moreover, deployment of the chimney stent before deployment of the endobags may result in inaccurate positioning of the main graft. However, it is yet unknown what will be the optimal sequence of steps regarding CG and endograft deployment.

A longer proximal sealing zone could have improved proximal graft apposition in the studied configurations, but the chosen geometry was based on real-life CT scans and thus clinically relevant. However, the average anatomy of 25 elective AAA patients was fairly straightforward, and results cannot be generalized for the entire population undergoing either ch-EVAR or ch-EVAS. The formation of gutters and compression of CG is likely influenced by a different geometry, and a phantom geometry including severe aortoiliac angulations and an asymmetric origin of branches would have been interesting to examine including the studied configurations. A patient-specific analysis, also including clinical outcomes, may be useful to assess clinical relevance of the findings.

In addition, geometry changes that may occur during the cardiac cycle were excluded, whereas the configurations were studied at static CT acquisitions. The flow distribution to branch vessels differed slightly from the intended flow, and also the systemic pressure was somewhat higher than the normal rest range, but flow distribution and pressure were still within a physiologic range. The models were fabricated from an elastic silicone. The models in this study may therefore be more elastic compared with in vivo, whereas aneurysms are usually stiffer because of a larger volume of collagen and less volume of elastin and muscle cells.[24]

CONCLUSIONS

This study showed that gutter volume is lowest in ch-EVAS with Viabahn stents. CG compression was lower in all configurations with Advanta V12 in comparison to Viabahn stents, but renal flow was unrestricted by CG compression. Further research is required to assess clinical implications of these findings concerning the incidence of type Ia endoleak and CG patency.

We would like to thank everyone of the Radiology Department at the Rijnstate Hospital who contributed to this study by assisting in planning of the implant sessions and image acquisition. In addition, we would like to thank ScoVas Medical BV for providing materials and assistance during implantation of the stent configurations in the models.

AUTHOR CONTRIBUTIONS

Conception and design: JB, ED, EGJ, MR
Analysis and interpretation: JB, RS, CS, JV, MR
Data collection: JB, ED, RS, SO
Writing the article: JB, JV, MR
Critical revision of the article: ED, EGJ, RS, SO, CS, JV, MR
Final approval of the article: JB, ED, EGJ, RS, SO, CS, JV, MR
Statistical analysis: JB, RS
Obtained funding: EGJ, MR
Overall responsibility: MR

REFERENCES

1. Stather P, Sidloff D, Dattani N, Choke E, Bown M, Sayers R. Systematic review and meta-analysis of the early and late outcomes of open and endovascular repair of abdominal aortic aneurysm. Br J Surg 2013;100:863-72.
2. Abbruzzese TA, Kwolek CJ, Brewster DC, Chung TK, Kang J, Conrad MF, et al. Outcomes following endovascular abdominal aortic aneurysm repair (EVAR): an anatomic and device-specific analysis. J Vasc Surg 2008;48:19-28.
3. Malina M, Resch T, Sonesson B. EVAR and complex anatomy: an update on fenestrated and branched stent grafts. Scand J Surg 2008;97:195-204.
4. AbuRahma AF, Campbell JE, Mousa AY, Hass SM, Stone PA, Jain A, et al. Clinical outcomes for hostile versus favorable aortic neck anatomy in endovascular aortic aneurysm repair using modular devices. J Vasc Surg 2011;54:13-21.
5. Antoniou GA, Georgiadis GS, Antoniou SA, Kuhan G, Murray D. A meta-analysis of outcomes of endovascular abdominal aortic aneurysm repair in patients with hostile and friendly neck anatomy. J Vasc Surg 2013;57:527-38.
6. Verhoeven EL, Vourliotakis G, Bos WT, Tielliu IF, Zeebregts CJ, Prins TR, et al. Fenestrated stent grafting for short-necked and juxtarenal abdominal aortic aneurysm: an 8-year single-centre experience. Eur J Vasc Endovasc Surg 2010;39:529-36.
7. Katsargyris A, Oikonomou K, Klonaris C, Topel I, Verhoeven EL. Comparison of outcomes with open, fenestrated, and chimney graft repair of juxtarenal aneurysms: are we ready for a paradigm shift? J Endovasc Ther 2013;20:159-69.
8. Resch TA, Sonesson B, Dias N, Malina M. Chimney grafts: is there a need and will they work? Perspect Vasc Surg Endovasc Ther 2011;23:149-53.
9. Greenberg RK, Clair D, Srivastava S, Bhandari G, Turc A, Hampton J, et al. Should patients with challenging anatomy be offered endovascular aneurysm repair? J Vasc Surg 2003;38:990-6.
10. Lee JT, Lee GK, Chandra V, Dalman RL. Comparison of fenestrated endografts and the snorkel/chimney technique. J Vasc Surg 2014;60:849-56; discussion: 856-7.
11. van den Ham LH, Zeebregts CJ, de Vries JP, Reijnen MM. Abdominal aortic aneurysm repair using Nellix EndoVascular Aneurysm Sealing. Surg Technol Int 2015;26:226-31.

12. Karthikesalingam A, Cobb RJ, Khoury A, Choke EC, Sayers RD, Holt PJ, et al. The morphological applicability of a novel endovascular aneurysm sealing (EVAS) system (Nellix) in patients with abdominal aortic aneurysms. Eur J Vasc Endovasc Surg 2013;46:440-5.
13. Malkawi AH, de Bruin JL, Loftus IM, Thompson MM. Treatment of a juxtarenal aneurysm with the Nellix endovascular aneurysm sealing system and chimney stent. J Endovasc Ther 2014;21:538-40.
14. Dijkstra ML, Lardenoye JW, van Oostayen JA, Zeebregts CJ, Reijnen MM. Endovascular aneurysm sealing for juxtarenal aneurysm using the Nellix device and chimney covered stents. J Endovasc Ther 2014;21:541-7.
15. Truijers M, van Sterkenburg SM, Lardenoije JW, Reijnen MM. Endovascular repair of a ruptured pararenal aortic aneurysm using the Nellix endovascular aneurysm sealing system and chimney grafts. J Endovasc Ther 2015;22:291-4.
16. Groot Jebbink E, Mathai V, Boersen JT, Sun C, Slump CH, Goverde PC, et al. Hemodynamic comparison of stent configurations used for aortoiliac occlusive disease [published online ahead of print October 12, 2016]. J Vasc Surg doi: 10.1016/j.jvs.2016.07.128.
17. Moore JE, Ku DN. Pulsatile velocity measurements in a model of the human abdominal aorta under resting conditions. J Biomech Eng 1994;116:337-46.
18. Yousif MY, Holdsworth DW, Poepping TL. A blood-mimicking fluid for particle image velocimetry with silicone vascular models. Exp Fluids 2011;50:769-74.
19. Mestres G, Uribe J, García-Madrid C, Miret E, Alomar X, Burrell M, et al. The best conditions for parallel stenting during EVAR: an in vitro study. Eur J Vasc Endovasc Surg 2012;44:468-73.
20. de Bruin JL, Yeung KK, Niepoth WW, Lely RJ, Cheung Q, de Vries A, et al. Geometric study of various chimney graft configurations in an in vitro juxtarenal aneurysm model. J Endovasc Ther 2013;20:184-90.
21. Niepoth WW, de Bruin JL, Lely RL, Wisselink W, de Vries JP, Yeung KK, et al. In vitro feasibility of a sac-sealing endoprosthesis in a double chimney graft configuration for juxtarenal aneurysm. J Endovasc Ther 2014;21:529-37.
22. Tran K, Ullery BW, Lee JT. Snorkel/chimney stent morphology predicts renal dysfunction after complex endovascular aneurysm repair. Ann Vasc Surg 2016;30:1-11.
23. Overeem SP, Boersen JT, Schuurmann RC, Groot Jebbink E, Slump CH, Reijnen MM, et al. Classification of gutter type in parallel stenting during endovascular aortic aneurysm repair [published online ahead of print October 12, 2016]. J Vasc Surg doi: 10.1016/j.jvs.2016.08.087.
24. He CM, Roach MR. The composition and mechanical properties of abdominal aortic aneurysms. J Vasc Surg 1994;20:6-13.

Submitted Jun 21, 2016; accepted Oct 2, 2016.

Additional material for this article may be found online at www.jvascsurg.org.

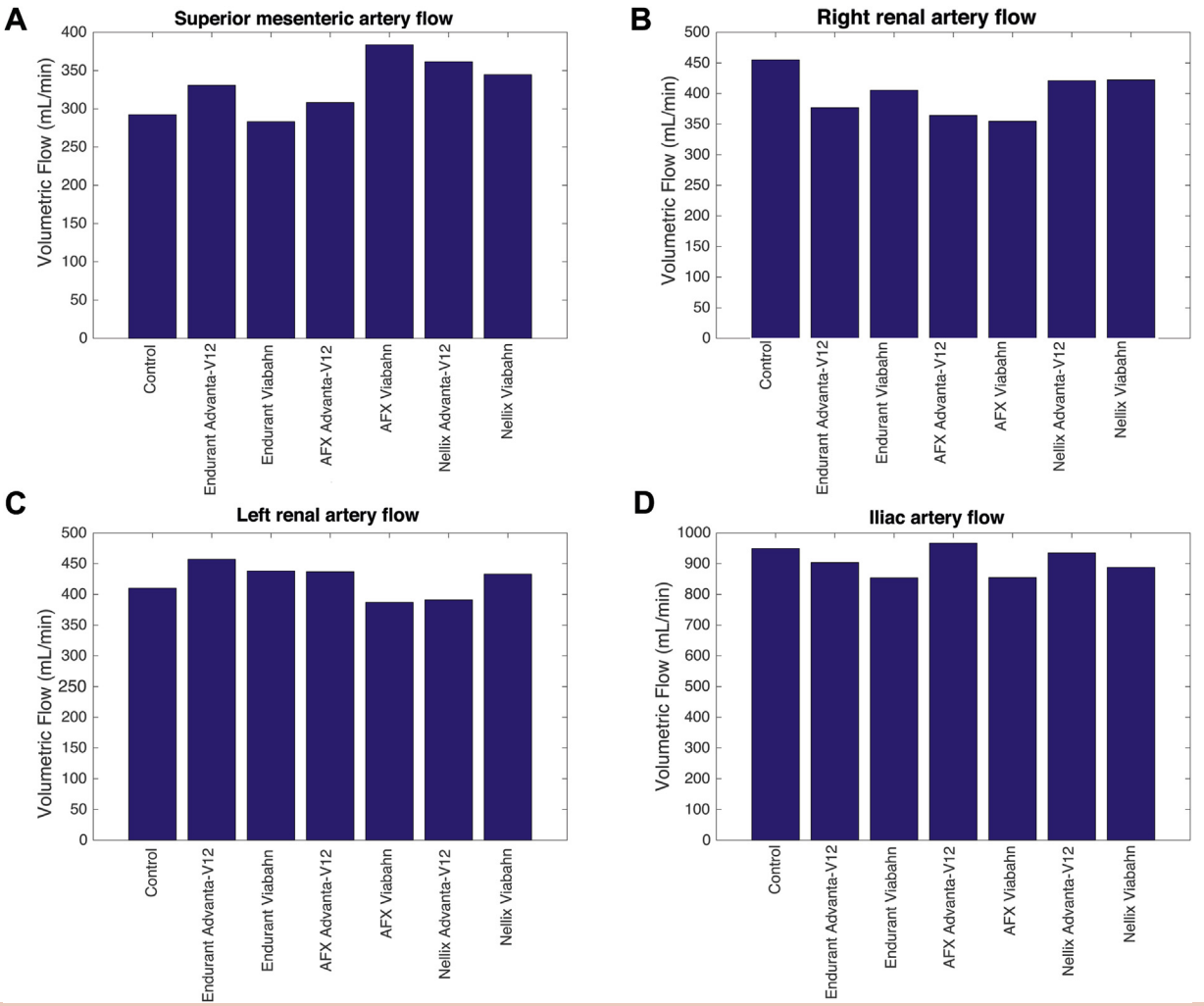

Supplementary Fig (online only). The average branch flow in the superior mesenteric artery (SMA), renal arteries, and common iliac artery for each configuration.